HHS Public Access

Author manuscript

Acta Biomater. Author manuscript; available in PMC 2018 March 15.

Published in final edited form as:

Acta Biomater. 2017 March 15; 51: 138–147. doi:10.1016/j.actbio.2017.01.012.

End-Point Immobilization of Heparin on Plasma-Treated Surface of Electrospun Polycarbonate-Urethane Vascular Graft

Xuefeng Qiu[1,2,3,*], **Benjamin Li-Ping Lee**[1,*], **Xinghai Ning**[1], **Niren Murthy**[1], **Nianguo Dong**[2], and **Song Li**[1,3,4,#]

[1]Department of Bioengineering, University of California, Berkeley, CA 94720, USA

[2]Department of Cardiovascular Surgery, Union Hospital, Tongji Medical School, Huazhong University of Science and Technology, Wuhan 430022, People's Republic of China

[3]Department of Bioengineering, University of California, Los Angeles (UCLA), Los Angeles, CA90095, USA

[4]Department of Medicine, University of California, Los Angeles (UCLA), Los Angeles, CA 90095, USA

Abstract

Small-diameter synthetic vascular grafts have high failure rate due to primarily surface thrombogenicity, and effective surface chemical modification is critical to maintain the patency of the grafts. In this study, we engineered a small-diameter, elastic synthetic vascular graft with off-the-shelf availability and anti-thrombogenic activity. Polycarbonate-urethane (PCU), was electrospun to produce nanofibrous grafts that closely mimicked a native blood vessel in terms of structural and mechanical strength. To overcome the difficulty of adding functional groups to PCU, we explored various surface modification methods, and determined that plasma treatment was the most effective method to modify the graft surface with functional amine groups, which were subsequently employed to conjugate heparin via end-point immobilization. In addition, we confirmed *in* vitro that the combination of plasma treatment and end-point immobilization of heparin exhibited the highest surface density and correspondingly the highest anti-thrombogenic activity of heparin molecules. Furthermore, from an *in vivo* study using a rat common carotid artery anastomosis model, we showed that plasma-heparin grafts had higher patency rate at 2 weeks and 4 weeks compared to plasma-control (untreated) grafts. More importantly, we observed a more complete endothelialization of the luminal surface with an aligned, well-organized monolayer of endothelial cells, as well as more extensive graft integration in terms of vascularization and cell infiltration from the surrounding tissue. This work demonstrates the feasibility of electrospinning PCU as synthetic elastic material to fabricate nanofibrous vascular

[#]Corresponding to: Song Li, Ph.D., Department of Bioengineering and Medicine, University of California, Los Angeles, 410 Westwood Plaza, 5121 Engineering V, Los Angeles, CA 90095, Tel: (310)206-5819, songli@ucla.edu.
[*]These authors contributed equally to this work.

grafts, as well as the potential to endow desired functionalization to the graft surface via plasma treatment for the conjugation of heparin or other bioactive molecules.

Graphical abstract

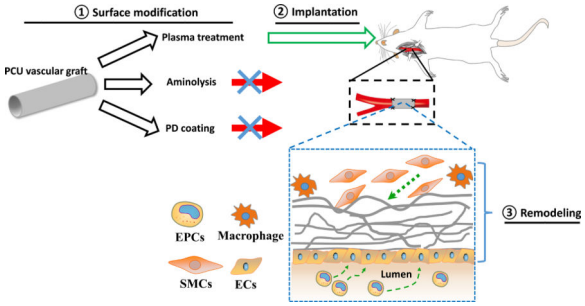

Vascular occlusion remains the leading cause of death all over the world, despite advances made in balloon angioplasty and conventional surgical intervention. Currently, autografts are the gold-standard grafts used to treat vascular occlusive disease. However, many patients with vascular occlusive disease do not have autologous vascular graft available. Therefore, there is a widely recognized need for a readily available, functional, small-diameter vascular graft (inner diameter of <6mm). This work addresses this critical need by developing a method of antithrombogenic modification of synthetic grafts.

Keywords

vascular grafts; electrospinning; polycarbonate-urethane; surface modification; plasma treatment; heparin

Introduction

Vascular diseases, specifically coronary and peripheral arterial diseases, affect millions of people and remain a worldwide problem as the prevalence continues to rise due to continued growth of the aging of the population (1). Thus, there is a major unmet need for small-diameter (< 6 mm) vascular grafts as bypass and blood vessel replacement, since autologous vessels, which represent the gold standard and have been shown to demonstrate superior clinical performance, are not always available (2–4). However, the success of synthetic grafts, such as ones made of Dacron (polyethylene terephthalate; PET) and Teflon (expanded polytetrafluoroethylene; ePTFE), is limited primarily to large-caliber vessels with high blood flow because of their surface thrombogenicity as well as poor elasticity and low compliance that cause acute thrombus formation and intimal hyperplasia, respectively (5–6). Similarly, despite the availability of commercially available heparin-coated synthetic vascular grafts, such as Propaten, that offer significantly better long-term patency over the standard ePTFE grafts but still has 63.5% failure rate after 48 months, the unmet need for small-diameter vascular grafts with low thrombogenicity still exists (7).

In order to address the shortcoming and develop an ideal, small-diameter vascular graft with mechanically compliant and anti-thrombogenic properties similar to those of native vessels,

different combinations that integrated unique *in vitro* endothelialization techniques or novel surface modifications to endow non-thrombogenic properties with synthetic (i.e. polyesters) as well as natural (i.e. decellularized) surfaces have been investigated (8–13). From a synthetic material perspective, many research groups have employed electrospinning to fabricate fibrous scaffolds for vascular regeneration, since fibrous structures obtained through electrospinning can be tailored to closely resemble the structure and function of the native extracellular matrix (ECM) in order to facilitate cell-material interactions (14–17). More importantly, such synthetic vascular grafts for small-diameter vessel applications are advantageous because they not only offer off-the-shelf availability but also reduce complications associated with donor-site morbidity and *in vitro* cell source and compatibility.

Recently, one particular polymer that has been electrospun to produce vascular grafts is polyurethane (18–20). Polyurethanes (PUs) possess excellent biocompatibility and more importantly mechanical properties, which make them ideal for vascular graft applications (21). However, despite their long-term biostability, PUs eventually degrade *in vivo*; polyester-based PU is susceptible to hydrolytic degradation in the body, whereas polyether-based PU is prone to oxidative degradation (22–24). As a result, polycarbonate-urethanes (PCUs) have gained more attention and have been used recently for their improved stability and resistance to both hydrolytic and oxidative degradation (25–27). Although PU grafts have been reported to have variable patency rates, which in some studies exhibited lower patency rates compared to ePTFE grafts (28, 29), the newer PCUs with and without modifications have reduced thrombogenicity and better *in vivo* performance (30, 31). More importantly, unlike ePTFE and Dacron, which are much stiffer and less compliant than native vessels, PCU better matches the mechanical properties of native vessels in terms of stiffness and compliance (32, 33).

Numerous strategies of surface modification have been explored to further improve the blood compatibility (i.e. conjugation of heparin) of these PCU surfaces, including chemical immobilization, physical adsorption, and plasma treatment. Heparin, a commonly used anticoagulant agent, has been utilized extensively in vascular therapies because of its ability to interact with anti-thrombin-III (AT-III) in preventing thrombus formation (34, 35). For example, we have previously shown that heparin-modified nanofibrous vascular grafts fabricated using biodegradable poly(L-lactide) (PLLA) exhibited higher patency and greater cell infiltration, suggesting that heparin may play multiple roles in maintaining function and promoting remodeling (36). Other chemical approaches to enable covalent conjugation of heparin using EDC chemistry range from bulk carboxylation of PU via bromoalkylation to the synthesis of PCU with pendant carboxyl groups or with PEG (20, 37, 38). In addition, recent findings on facile surface modification using mussel-inspired dopamine indicated that such passively adsorbed coating could not only enhance endothelial cell adhesion and viability but also immobilize biomolecules such as VEGF on the surface of vascular graft for accelerated endothelialization (39, 40). Because this adhesive polydopamine coating serves as a primer for further biofunctionalization, it can be easily applied to different polymeric surfaces for various applications (41, 42). Furthermore, plasma treatment has been utilized to modify the surface properties of PU as well. For instance, an early study by Kawamoto et al. demonstrated that plasma treatment altered the wettability of the surface of segmented-

polyurethane, making it more favorable for the adhesion and proliferation of bovine aortic endothelial cells (43). Similarly, Bae et al. used oxygen plasma glow discharge to prepare carboxyl group-introduced PU for coupling of polyethylene oxide to immobilize heparin (44). Although one disadvantage of plasma treatment is its limited penetration depth, the porous electrospun fibers can enhance the penetration, and it is a powerful surface modification technique useful for the development of small-diameter vascular graft in that surface features can be manipulated to facilitate subsequent biofunctionalization as well as desired endothelialization.

In this study, we electrospun and fabricated small-diameter nanofibrous vascular grafts using Carbosil®, a commercially available thermoplastic PCU. We then explored and selected three common surface modification techniques from an array of options, and investigated which of them would provide the most effective modification as a primer for subsequent immobilization of heparin on the surface of our PCU grafts. Specifically, we utilized aminolysis with 1-Ethyl-3-[3-dimethylaminopropyl]carbodiimide hydrochloride (EDC) chemistry as a chemical immobilization, polydopamine coating as a passive adsorption, and plasma treatment paired with end-point immobilization to initially introduce amine functional groups and ultimately conjugate heparin on the graft surface. After comparing the three methods, we determined the most effective modification with respect to the surface amine density as well as the anti-thrombogenic activity of the immobilized heparin. Lastly, we proceeded with these optimized PCU grafts immobilized with heparin for short-term *in vivo* studies, focusing on the performance of heparin-modified electrospun PCU grafts on graft patency as well as endothelialization and overall biocompatibility.

Materials and Methods

Fabrication and Characterization of Polycarbonate-Urethane (PCU) Nanofibrous Vascular Graft

Electrospinning was performed as previously described with minor modification to produce polycarbonate-urethane (PCU) vascular graft (36, 45). Briefly, polycarbonate-urethane (Carbosil® 90A, DSM Biomedical, Berkeley, CA) was dissolved via sonication in dimethylformamide (DMF) at 16.5% (w/v) concentration. To deliver the polymer solution, a programmable pump along with a 5 mL syringe, which was fitted with flexible silicon tubing connected to 1.5-inch long stainless steel 23G dispensing needles, was used. Two high-voltage generators were utilized to apply approximately +9.7 kV voltage to the needle and −9.2 kV voltage to the collecting mandrel. In addition, the humidity was controlled to be 50–52% during the electrospinning process. PCU solution was delivered at a flow rate of 1.05 mL/hr and gap distance (distance between the positively charged needle tip and the negatively charged collecting mandrel) of 16.5 cm, with a spinneret that traversed in the longitudinal direction to achieve a uniform thickness of the graft longitudinally. PCU fibers with random orientation were obtained by using a low rotation speed (100 rpm) for the collecting mandrel. Electrospinning was allowed to proceed until the wall of the vascular graft reached a desired thickness based on measurements with a thickness gauge (Mitutoyo America, Aurora, IL). The finished graft was placed in a chemical hood overnight to remove any residual DMF.

The overall fibrous structure and integrity of the PCU graft were inspected and imaged using scanning electron microscopy (SEM; TM-1000, Hitachi, Pleasanton, CA). In addition, to determine the mechanical properties of the electrospun PCU graft, graft segments of 1 mm in diameter and 1.5–2 mm in width were prepared and subjected to uniaxial tensile testing in the radial direction using an Instron 5544 tester (Instron, Canton, MA) as described previously (46). Briefly, two 0.3-mm-diameter stainless steel wires were placed through the lumen of the ring segment of the graft and loaded in between the grips. Each segment was extended until failure at a rate of 0.1 mm/sec, and the applied force and deformation was recorded via Bluehill software (Instron Corp.). The elastic modulus was calculated based on the applied load, deformation, and dimensions (thickness and width) of the graft segments; the ultimate tensile strength was recorded as the peak stress prior to failure. The same procedure was conducted after each chemical modification to assess potential changes in the mechanical properties of the PCU graft.

Aminolysis of PCU vascular graft to introduce amine functional groups for heparin conjugation

We modified the aminolysis procedure as reported by Zhu et al. to introduce functional amine groups onto the surface of our polycarbonate-urethane (PCU) vascular graft (47). Briefly, PCU vascular grafts were aminolyzed by immersing them in 100% ethanol (EtOH) containing 50 mg/mL 4-arm-amine-Polyethylene glycol (PEG) (Sunbright PTE-050PA, NOF America Corporation, White Plains, NY), and heated at 60°C for approximately 4 hours. Aminolyzed grafts were subsequently washed thoroughly with 70% EtOH followed by distilled water. Fourier transform infrared (FTIR) spectrometry was performed with a FTIR spectrometer (Nicolet Avatar 360, Thermo Fisher Scientific, Waltham, MA) as described previously to verify the presence of amine functional groups on the graft surface (data not shown) (48). Lastly, 30 mg/mL of unfragmented heparin sodium (Sigma Aldrich, St. Louis, MO) was covalently conjugated to the free amines on the surface of aminolyzed grafts via EDC and Sulfo-NHS (Pierce Biotechnology, Rockford, IL) as described previously (49). These heparin-conjugated grafts via aminolysis will be referred to as aminolysis-heparin grafts in the remainder of this study.

Polydopamine coating of PCU vascular graft for passive heparin adsorption

We modified the polydopamine coating procedure as described by Lee et al. to introduce an adhesive surface capable of immobilizing biomolecules (50). Briefly, PCU vascular grafts were initially immersed in 100% EtOH for approximately 10 minutes and washed thoroughly using 1X PBS (pH 8.3). They were then immersed in 2.0 mg/mL of dopamine hydrochloride (Sigma Aldrich) prepared in PBS (pH 8.3) overnight on a shaker at room temperature, and washed with PBS and dried with nitrogen gas. The formation of the polydopamine coating on the grafts was confirmed visually as well as using water contact angle measurements (data not shown). Prior to heparin conjugation, polydopamine-coated grafts were immersed in 0.1N NaOH for 5 minutes and washed with PBS (pH 9). They were subsequently immersed in 30 mg/mL heparin solution prepared in PBS (pH 9) for 24 hours on a shaker at room temperature, followed by washes with PBS. These heparin-adsorbed grafts via polydopamine coating will be referred to as polydopamine (PD)-heparin grafts in the remainder of this study.

Plasma treatment of PCU vascular graft to introduce amine functional groups for end-point immobilization of heparin

With the assistance of Plasma Technology Systems (Belmont, CA), amine functionality was achieved on the graft surface using a two-stage gas plasma recipe from Plasmatreat's Aurora™ low-pressure plasma reactor. The plasma reactor is configured with two side-wall electrodes. A 500-watt RF generator delivers power to the electrodes at 13.56 Mhz. PCU grafts were treated atop Whatman™ glass microfiber filter suspending on screen trays spanning between the power electrodes. The two stages of the plasma recipe consisted of an O_2 plasma cleaning for 1 minute followed by an allylamine plasma vapor for 9 minutes to allow polymerization and create an ultra-thin film of stable primary and secondary amines on the graft surface. The allyl-amine evaporation was assisted by a 70°C hot tube and liquid injection system. FTIR spectrometry was performed to confirm the presence of amine functional groups on the graft surface (data not shown). Heparin was conjugated via end-point immobilization onto the surface of plasma-treated grafts, since each heparin chain contains a reducing-end hemiacetal that can be covalently attached to the free amines on the graft surface through reductive amination (51, 52). Specifically, as previously described with minor modifications, the plasma-treated grafts were immersed in 30 mg/mL heparin solution prepared in cyanoborohydride coupling buffer (0.02 M sodium phosphate, 0.2 M sodium chloride, and 3 mg/mL sodium cyanoborohydride; pH 5.5) for 24 hours on a shaker at room temperature, followed by PBS washes (53). These heparin-conjugated grafts via plasma treatment will be referred to as plasma-heparin grafts in the remainder of this study.

Utilization of Orange II and Coomassie Brilliant Blue (CBB) Assays for Amine Detection and Quantification

Two colorimetric assays were used as previously described with minor modifications to quantify the amount of free amine groups on the modified surfaces (via aminolysis, polydopamine, and plasma treatment) of the PCU vascular grafts: Orange II and Coomassie Brilliant Blue (CBB) (54). For both methods, standard solutions containing 0 to 20 mg of NovaPEG amino resin (Novabiochem/EMD Millipore, Billerica, MA) were prepared and used to determine the amine density on the graft surface based on absorbance value comparisons.

Orange II—Modified PCU grafts (1-mm diameter, 0.5-cm length) were immersed in Orange II dye solution (14 mg/mL, Sigma Aldrich) in acidic solution (distilled water adjusted to pH 3 with 1 M HCl) for 30 minutes at 40°C. The grafts were thoroughly and carefully washed using the acidic solution (pH 3) to remove all unbound dye. After air-drying overnight, the grafts were immersed in 1 mL of alkaline solution (distilled water adjusted to pH 12 with 1M NaOH solution). Subsequently, the pH of the solution containing the desorbed dye was adjusted to pH 3 using HCl. The absorbance of the solution from each modification method was measured at 490 nm (Molecular Devices ThermoMax, GMI Inc., Ramsey, MN) and recorded.

Coomassie Brilliant Blue (CBB)—Modified PCU grafts were immersed in Coomassie Blue dye solution (0.5 mg/mL, Sigma Aldrich) in acidic solution (approximately 85:10:5 v/v distilled water/methanol/acetic acid; pH ~2.3) for 5 minutes at room temperature. The

samples were thoroughly and carefully washed using the same acidic solution to remove all unbound dye. After air-drying overnight, the grafts were immersed in alkaline solution (0.125 M potassium carbonate in 50:50 v/v distilled water/methanol; pH 11.25). The pH of the solution containing the desorbed dye was subsequently adjusted to pH 3 by adding HCl. The absorbance of the solution from each method was then measured at 650 nm (Molecular Devices ThermoMax) and recorded.

Quantification of Heparin on Heparin-Conjugated PCU Vascular Grafts to Determine Its Anti-thrombogenic Activity and Stability

The presence and stability of heparin on the heparin-conjugated PCU grafts modified via aminolysis, polydopamine, and plasma treatment was confirmed and measured by using toluidine blue (Sigma Aldrich) as described previously (36). Briefly, at day 0 (immediately after heparin conjugation) and day 7 (one week post-heparin conjugation in which grafts were placed in PBS at room temperature on a shaker), control (untreated), aminolysis-heparin, PD-heparin, and plasma-heparin grafts were immersed in 0.0005% (w/v) toluidine blue solution and vortexed for 10 minutes. Heparin standard solutions containing different amounts of heparin were also prepared in 0.0005% (w/v) toluidine blue solution and vortexed for 10 minutes. After vortexing, 3 mL of n-hexane was added to all the heparin standard and sample solutions and vortexed again for 30 seconds to extract the unbound toluidine blue. The absorbance of the unbound toluidine blue was subsequently measured at 650 nm (Molecular Devices ThermoMax) and recorded. The density of immobilized heparin on all the samples was determined by comparing their absorbance values to those of the heparin standard solutions.

The anti-thrombogenic activity and stability of heparin-conjugated PCU grafts modified via aminolysis, polydopamine, and plasma treatment were determined by measuring thrombin activity with the chromogenic substrate S-2238 (Diapharma, West Chester, OH) in the presence of anti-thrombin-III (AT-III) as previously described with minor modification (36). Similar to the toluidine blue assay, control (untreated), aminolysis-heparin, PD-heparin, and plasma-heparin grafts taken from day 0 and day 7 were incubated in a 50 mM Tris buffer along with 0.08 NIH units of human AT-III (Sigma Aldrich) for 5 minutes at 37°C. Heparin standard solutions containing varying amounts of heparin were also prepared in Tris buffer along with 0.08 NIH units of human AT-III. Subsequently, 0.08 NIH units of human thrombin (Sigma Aldrich) were added to each of the samples and standard solutions, followed by mixing and incubating for 30 seconds at 37°C. After the thrombin addition, 5 mM S-2238 was added to the samples and standard solutions, which were then incubated for 8 minutes at 37°C. Lastly, all the reactions were stopped by adding 40% acetic acid. The absorbance of the sample supernatants as well as the standard solutions were measured at 405 nm (Molecular Devices ThermoMax) and recorded to determine the thrombin activity in the solutions. The heparin activity of all the samples was subsequently determined by comparing the absorbance values to those of the heparin standard solutions.

Implantation and explantation of plasma-treated PCU vascular grafts

All experimental procedures were approved by the Institutional Review Board Service and the Institutional Animal Care and Use Committee (IACUC) at the University of California,

Berkeley. To evaluate and compare the performance of control (untreated) and heparin-conjugated PCU grafts in a short-term *in vivo* study, we used a rat common carotid artery anastomosis model. Male Sprague-Dawley (SD) rats were purchased from the Charles River animal facility. Prior to implantation, 1 mm-diameter PCU grafts were electrospun, plasma treated, and disinfected with 70% EtOH under germicidal UV for 10 minutes (referred to as plasma-control grafts); for heparin-conjugated grafts, they were subsequently conjugated with heparin via reductive amination as aforementioned (referred to as plasma-heparin grafts). The rats were anesthetized with 2% isoflurane in 70% nitrous oxide and 30% oxygen. The left common carotid artery was dissected, clamped, and transected. The graft (approximately 1.0 cm in length) was then sutured end to end with 8 interrupted stitches by using a 10-0 needle. No heparin or any other anticoagulant was used at any point before, during, or after the implantation procedure. Each group at each time point included 7 animals (n=7). To determine patency of the graft at the time of explantation after 2 weeks and 4 weeks *in vivo*, the blood flow in the blood vessel at the distal anastomosis was examined and verified in the live animal under anesthesia. Specifically, the graft was defined as being patent if unobstructed blood flow and noticeable pulsation were observed through the graft and the distal carotid artery. Lastly, the animals were euthanized, and the vascular grafts were explanted and immediately processed for *en face* immunofluorescent staining of the luminal (inner) graft surface or histological analysis and immunofluorescent staining.

Histological analysis and immunofluorescence staining

For *en face* immunofluorescent staining of the luminal (inner) graft surface, the explanted grafts were carefully trimmed longitudinally using microscissors into four (quarter) pieces and fixed with 4% paraformaldehyde (PFA) for 30 minutes. The samples were then washed with PBS, permeabilized with 0.5% Triton X-100, and blocked with 5% donkey serum. Subsequently, they were stained with the following primary antibodies: CD31 (rabbit, Abcam Inc., Cambridge, MA), CD34 (AF4117, goat, R&D Systems, Littleton, CO), vWF (SC-14014, rabbit, Santa Cruz Biotechnology Inc.), and CD45 (05-1410, mouse, EMD Millipore, Billerica, MA). The samples were stained with DAPI for cell nuclei. Images were captured with a Swept Field Confocal (SFC) microscope (Prairie Technologies, Middleton, WI).

Explanted samples for histological analysis were immediately fixed with 4% PFA before being snap-frozen and embedded in optimal cutting temperature (OCT) compound (TissueTek, Elkhart, IN). Cross-sections of 12-μm thickness were collected using a cryosectioner. For immunofluorescent staining, the samples were fixed with 4% PFA, permeabilized with 0.5% Triton X-100, and blocked with 5% donkey serum. They were subsequently stained with the same primary antibodies listed previously in addition to: SMA (ab7817, mouse, Abcam Inc.), CD68 (MCA341R, mouse, AbD Serotec, Raleigh, NC), and CD163 (MCA342R, mouse, AbD Serotec). Lastly, they were stained with DAPI, followed by confocal microscopy with a Zeiss LSM710 confocal microscope (Carl Zeiss, Inc., Thornwood, NY).

Statistical Analysis

The data in this study are presented as mean ± standard deviation. For comparison between two groups, two-tailed Student's *t*-test was used. For multiple pairwise comparisons to detect whether a significant difference existed between groups with different treatments, all data were initially compared using analysis of variance (ANOVA), followed by Holm's *t*-test for post-analysis. Fischer exact test was used to analyze the patency data. A P-value of less than 0.05 between samples in comparison was considered statistically significant.

Results and Discussion

Structural and Mechanical Characterization of PCU Vascular Grafts

We examined the fibrous architecture and quality of our electrospun PCU vascular graft (1.0 mm in internal diameter, 130±5 μm in wall thickness) via SEM (Figure 1A–D). The PCU fibrous structure consisted of individual fibers with diameters ranging from approximately 160 nm to 2 μm, with an average fiber diameter of 497 ± 316 nm (n=50). As depicted in the micrographs, the fibrous structure of both the inner (luminal) and outer surfaces of the graft were shown in Figure 1C and Figure 1D, respectively. The fibrous structures of both the inner and outer surfaces of the graft were shown in Figure 1E and Figure 1F after the plasma treatment. In addition, desirable porosity as well as random structure and orientation of fibers were achieved, confirming the uniformity and consistency in our optimized parameters for electrospinning PCU. In fact, the parameters were able to produce quality grafts of varying diameters (i.e. 1 mm and 6 mm) that exhibited uniform wall thickness, surface appearance, and overall graft properties (Figure 1E,F), demonstrating the versatility of our electrospinning setup.

Mechanical strength plays a major role in dictating the long-term stability of vascular grafts. Specifically, compliance mismatch at the end-to-end anastomosis between the native artery and the rigid synthetic, especially Dacron and ePTFE, graft results in disturbed flow and shear stress. Thus, we performed mechanical tests to compare our electrospun PCU grafts treated with different chemical modifications and evaluate whether they exhibited similar properties as those of native arteries in terms of elastic modulus and tensile strength (Figure 1G). Based on our measurements, control (untreated) PCU grafts had an elastic modulus of 2.5 ± 0.1 MPa, which is slightly lower than that of the aminolyzed (2.6 ± 0.1 MPa) and polydopamine-coated (3.0 ± 0.4 MPa) grafts. Interestingly, the elastic modulus of plasma-treated grafts (3.9 ± 0.2 MPa) was significantly higher than the control as well as the aminolysis- and polydopamine-modified grafts. It is possible that our surface plasma treatment had a strengthening effect, which could be explained by the increase in elastic modulus of individual fibers or potential interfacial adhesion between adjacent fibers (55, 56). On the other hand, the control grafts exhibited an ultimate tensile strength of 6.5 ± 0.4 MPa, comparable to that of the aminolyzed (6.3 ± 0.7 MPa), polydopamine-coated (7.4 ± 1.1 MPa), and plasma-treated (6.5 ± 0.2 MPa) grafts. The comparison of these values indicated that each of the chemical modifications used in this study to functionalize the PCU graft did not adversely affect the overall structure and integrity but could rather strengthen the graft, especially in the case of plasma treatment. More importantly, these tensile strengths are higher than those of the rat common carotid arteries, which have been

characterized to be approximately 1.8 ± 0.1 MPa (57). However, the mechanical properties of the PCU graft may be further tailored for different applications, such as utilization as conduits for nerve regeneration, by manipulating fabrication parameters and fiber orientation.

Chemical Characterization of Surface Modification of PCU Vascular Grafts

Since mechanical characterization to compare the three chemical modifications did not reveal any undesired changes in mechanical properties, we utilized two chemical assays to assess their effectiveness in amine functionalization of the graft surface: Orange II and CBB. Both dyes are commonly used for primary amino group quantification, as they are less expensive, less time-consuming, and more quantitative than other methods, including fluorometry, colorimetry, and spectroscopy. After using varying amounts of the NovaPEG amino resin with known surface amine density to generate a standard curve for each of the two dyes, we quantified the density of exposed primary amine groups on the graft surface (with same dimensions) modified with the different methods (Figure 2A, B). For the control (untreated) graft, an insignificant Orange II concentration (0.37 ± 0.04 mmol/cm^3) was detected, suggesting that nonspecific interactions between the dye and the PCU surface were minimal. In contrast, the plasma-treated graft had an Orange II concentration of 29.8 ± 0.1 mmol/cm^3, significantly higher than the control as well as the aminolyzed graft (3.6 ± 0.1 mmol/cm^3) and PD-coated graft (13.7 ± 0.2 mmol/cm^3) (Figure 2A). Similarly, the same trend was observed using the CBB dye, in which the concentration of the dye on the plasma-treated graft (46.9 ± 0.5 μmol/cm^3) was significantly higher than the negligible amount on the control (0.003 ± 1.2 μmol/cm^3) as well as the much lower concentrations on the aminolyzed graft (10 ± 3 μmol/cm^3) and PD-coated graft (28.5 ± 0.6 μmol/cm^3) (Figure 2B). Although the exact amine densities as determined by the two colorimetric methods did not match, in which the values from the CBB method were drastically lower than those from the Orange II method, the results were consistent with findings reported previously in a comparison study (54). In fact, because CBB is a large divalent dye, there exists steric hindrance between CBB molecules that prevented them from binding to some amine groups on the graft surface, resulting in much lower values and lower surface binding compared to those of the small monovalent Orange II dye. Despite the quantitative difference between the Orange II and CBB methods, both revealed the same trend that strongly supported the effectiveness of functionalizing the PCU surface via plasma treatment in comparison to aminolysis and polydopamine coating, specifically in introducing amine groups that could be utilized for subsequent biofunctionalization, such as heparin conjugation.

Verification of Heparin Modification of PCU Vascular Grafts

To further demonstrate that the significantly higher amine density on the plasma-treated PCU graft corresponded to better heparin conjugation with respect to heparin density and stability, we utilized toluidine blue assay to verify and quantify the immobilized heparin on the modified grafts at day 0 (immediately) and day 7 (one week) after heparin immobilization (Figure 2C). Immediately after heparin conjugation at day 0, control (untreated) grafts had an insignificant amount of heparin (2.5 ± 0.1 μg/cm^3) compared to the heparin density on aminolysis-heparin (27 ± 11 μg/cm^3), PD-heparin (28 ± 27 μg/cm^3), and plasma-heparin (48 ± 15 μg/cm^3) grafts, confirming that heparin was successfully

conjugated via all three methods to the nanofibers. In fact, heparin density on aminolysis-heparin and plasma-heparin grafts was significantly higher than that of control. On the other hand, one week (day 7) after initial heparin conjugation, heparin density on the control, aminolysis-heparin, PD-heparin, and plasma-heparin grafts was 1.2 ± 0.7 μg/cm^3, 22 ± 18 μg/cm^3, 21 ± 11 μg/cm^3, and 43 ± 6 μg/cm^3, respectively. Even though heparin density on both PD-heparin and plasma-heparin grafts was significantly higher than that of control, plasma-heparin grafts retained significantly more heparin than PD-heparin grafts, indicating that plasma treatment was able to bind the most heparin without compromising the stability of the immobilized heparin. This could be correlated with the highest amine density on the surface of plasma-treated grafts, but we speculated that the end-point immobilization of heparin also contributed to the highest heparin density on plasma-heparin grafts because cross-linking may likely decrease the available surface area for heparin attachment. In addition, we believe that the more noticeable decrease in heparin density on the aminolysis-heparin and PD-heparin grafts after one week was due to the loss of heparin that was loosely and not covalently attached to the surface via nonspecific binding. In order to confirm these speculations, more in-depth analyses need to be further conducted to elucidate the ratio of nonspecific binding and cross-linking as well as the orientation of bound heparin.

Detection of Heparin Activity of Modified PCU Vascular Grafts

At day 0, control grafts exhibited a baseline activity level of 0.8 ± 0.4 NIH U/cm^3 (Figure 2D). This value was minimal and significantly lower compared to the activity levels of aminolysis-heparin (8.0 ± 0.1 NIH U/cm^3), PD-heparin (8.4 ± 0.3 NIH U/cm^3), and plasma-heparin (8.2 ± 0.4 NIH U/cm^3) grafts, confirming that the successfully immobilized heparin via the three modifications showed high levels of anti-thrombogenic activity. However, at day 7, control, aminolysis-heparin, PD-heparin, and plasma-heparin exhibited activity levels of 0.50 ± 0.03 NIH U/cm^3, 3.6 ± 0.2 NIH U/cm^3, 4.4 ± 0.3 NIH U/cm^3, and 8.3 ± 0.2 NIH U/cm^3, respectively. Consistent with our previous results from toluidine blue assay, the heparin conjugated via end-point immobilization on the plasma-treated surface was the most stable as it retained significant activity. In comparison, heparin activity of control, aminolysis-heparin, and PD-heparin groups significantly decreased after 7 days. This suggests that end-point immobilization is more effective and advantageous in that the heparin molecules were immobilized in a more favorable and accessible orientation on the surface of plasma-heparin grafts, thus maximizing the exposure and availability of AT-III binding sites on the immobilized heparin (52, 58). Therefore, the combination of plasma treatment for amine functionalization and end-point immobilization for heparin attachment provided the most effective technique for heparin conjugation in terms of surface amine functionalization and the maintenance and retention of heparin activity on our electrospun PCU grafts, which was thus selected and used for subsequent small-animal studies to evaluate performance *in vivo*.

In Vivo Performance and Patency of PCU Vascular Grafts

One strategy to improve preclinical and clinical outcomes of synthetic vascular grafts is to incorporate heparin as a blood-contacting coating. Because of its desired anticoagulant and anti-thrombogenic properties, heparin has been reported to improve the patency of small-diameter grafts (29, 52). Thus, we aimed to test the efficacy of our surface amine

functionalization via plasma treatment by assessing the effects of heparin conjugation on the patency of PCU vascular grafts *in vivo*. Plasma-control (untreated) and plasma-heparin grafts with an inner diameter of 1 mm and approximate length of 1.0 cm were implanted into the left common carotid artery of SD rats. The grafts were examined at 2 weeks and 4 weeks post-operative procedure, with 7 animals per group for each time point. Images of a representative graft from each group at the two time points were taken immediately prior to explantation (Figure 3A–D). We noticed much more surrounding tissue around the grafts, especially the plasma-heparin grafts, with visible microvessels indicative of vascularization. Because heparin was immobilized to the entire graft surface during incubation in heparin solution, we believe that heparin may have played a major role in the recruitment of host cells and the development of such vascularized surrounding tissue. In fact, heparin has been well-reported to bind and regulate the activities of numerous proteins in cellular microenvironment, such as growth factors and ECM components, as well as cell surface proteins that together govern morphogenesis and tissue repair (59, 60). In terms of graft performance, at 2 weeks, approximately 71% (5 of 7) of plasma-control grafts remained patent, whereas 86% (6 of 7) of plasma-heparin grafts were patent. However, after 4 weeks, plasma-control grafts exhibited approximately 29% (2 of 7) patency, compared to 86% (6 of 7) patency of plasma-heparin grafts. As expected, the anti-thrombogenic activity of the immobilized heparin as confirmed through our *in vitro* assessment prevented occlusion as a consequence of acute thrombosis, which is a common mechanism for the failure of small-diameter grafts. Furthermore, our results (Figure 3E) showed that the difference in patency between heparinized and control groups was not significant at 2 weeks, but approaches significance by week 4 (P=0.051). These results showed interesting similarities and trends as reported in our previous studies (36, 49). Our approach confirmed a synergistic effect of heparin in combination with the nanofibrous structure of our PCU vascular grafts, as the benefits of heparin conjugation were more pronounced as a result of higher surface density from not only high surface-area-to-volume ratio of electrospun fibrous structure but also end-point immobilization of heparin molecules. Therefore, our heparin modification was effective at preventing thrombosis that would have delayed or prohibited endothelialization of the graft lumen.

Recruitment of Endogenous Progenitor Cells for Endothelialization and Graft Integration

In addition to mechanical properties, another critical element in dictating the success of vascular grafts *in vivo* is endothelialization. As a result, extensive research in the development and enhancement of an ideal, synthetic vascular graft has focused on engineering luminal surfaces that can promote and accelerate the formation of a mature and functional endothelium. We have previously shown that heparin-modified nanofibrous vascular grafts exhibited more complete endothelialization of the lumen compared to untreated grafts, suggesting that heparin modification may assist in the function and integration of vascular grafts *in vivo* (36). Similarly, results from our short-term *in vivo* studies were consistent with our previous findings.

En face immunostaining was performed to characterize the cells on the luminal surface of the grafts (Figure 4). Two patent grafts of 7 samples at each time point were used for *en face* immunostaining. At 2 weeks, plasma-heparin grafts (Figure 4: C, D) had noticeably more

cells in the middle portion of the grafts compared to plasma-control grafts (Figure 4: A, B). In fact, many of these cells were positive for CD34, a marker expressed by endothelial progenitor cells (EPCs). Several endothelial cells (ECs) as identified by $CD31^+$ and vWF^+ staining were also present. However, these ECs exhibited a more disorganized morphology and less defined cell-cell boundaries, indicating that endothelialization was incomplete as a stable endothelium was still in the early stage of formation. In addition, even though plasma-heparin grafts appeared to have attracted more cells, specifically EPCs, plasma-control grafts exhibited better than expected cell attachment and recruitment. We speculated that the change of PCU surface property from innately hydrophobic to hydrophilic as a result of plasma treatment facilitated cell adhesion, which is consistent with our previous finding that functional amine groups from Ar-NH_3/H_2 plasma treatment promoted attachment and spreading of bovine aorta endothelial cells (61). Furthermore, both plasma-control and plasma-heparin grafts had a small number of peripheral blood mononuclear cells positive for CD45 (Figure 4: B, D), reflecting a neglegible inflammatory response.

On the other hand, at 4 weeks after implantation, the luminal surface of the plasma-heparin graft was almost completely covered by cells (Figure 4: G–H). In particular, most of these cells were $CD31^+$ and vWF^+, with no $CD34^+$ cells present amongst the ECs. These ECs now exhibited a well-organized, cobblestone-like structure that closely resembled the endothelium of a native vessel, along with near-complete alignment of cell nuclei and morphology in the direction of blood flow. Nevertheless, further studies are needed to better determine whether such confluent endothelial coverage resulted from the differentiation and maturation of EPCs, which were observed to have attached at the 2-week time point, into ECs, or the proliferation of mature ECs that migrated trans-anastomotically. Moreover, as shown in Figure 4G–H, no $CD45^+$ cells were found in the 4-week plasma-heparin graft, suggesting that the inflammatory response was acute and transient in the presence of heparin.

SMA staining revealed that there were very few SMA^+ cells in the plasma-control and plasma-heparin grafts at the 2-week time point (Figure 5A, C). At 4 weeks, more SMA^+ cells were found migrating through the outer surface in plasma-heparin grafts than that in the plasma-control grafts (Figure 5 B, D). This observation is consistent with our previous findings that heparin modification of nanofibers enhance cell infiltration (61).

In terms of inflammatory response, we also performed cross-section staining for CD68 and CD163, which are markers of pan macrophages and specifically M2 macrophages, respectively. At 2 weeks, very few macrophages were found in the grafts and the surrounding tissue of the grafts (Figure A–D). At 4 weeks, more $CD68^+$ cells were present around the plasma-control graft than around the plasma-heparin graft (Figure 6E, G). Furthermore, our staining of CD163, indicative of M2 macrophages that have been shown to participate in tissue remodeling (62), showed some positive cells in the tissue surrounding both the plasma-control and plasma-heparin grafts after 4 weeks *in vivo* (Figure 6F, H). In general, electrospun PCU grafts showed low immune responses and did not recruit large number of macrophages.

Conclusion

In this study, we successfully developed small-diameter nanofibrous vascular grafts using a thermoplastic polycarbonate-urethane. These electrospun grafts possessed fibrous structure as well as mechanical strength, specifically elastic modulus and ultimate tensile strength, that closely mimic those of the native vessels. We then showed that desired surface functionalization could be achieved using plasma treatment, a technique that we demonstrated to be significantly more effective compared to alternative methods such as aminolysis and physical adsorption via polydopamine coating. In addition, these functional amine groups grafted on the graft surface were used for subsequent conjugation of heparin. In fact, plasma treatment followed by reductive amination permitted end-point immobilization of heparin molecules on the graft surface, providing not only higher surface density but more importantly better stability and anti-thrombogenic activity. Furthermore, from our short-term *in vivo* study, we demonstrated that the end-point immobilized heparin drastically improved the performance of the vascular grafts with respect to patency as well as early stages of endothelialization and graft integration. However, because rodents re-endothelialize synthetic grafts much more readily than humans do, additional studies may be done with vascular grafts of longer length and/or different animal models. Therefore, this engineering approach combined with optimal surface modification can serve as a foundation to develop small-diameter vascular grafts that possess off-the-shelf availability and desired bioactivity, which will have translational impact on the clinical treatment of vascular diseases.

Acknowledgments

This work is supported in part by the grants from the National Institute of Health (HL117213 and HL121450 to S.L.), California Institute of Regenerative Medicine (a clinical fellow's training grant TG2-01164 to X.Q.), National Natural Science Foundation of China (81170110/H0203 to X.Q.) and National Key R&D Plan (2016YFA0101100 to N.D.)

References

1. Kochanek K, Murphy S, Miniño A, Kung H. Deaths: final data for 2009. Natl Vital Stat Rep. 2011; 60(3):1–117.
2. Faries PL, LoGerfo FW, Arora S, Hook S, Pulling MC, Akbari CM, Campbell DR, Pomposelli FB Jr. A comparative study of alternative conduits for lower extremity revascularization: All-autogenous conduit versus prosthetic grafts. Journal of Vascular Surgery. 2000; 32(6):1080–1090. [PubMed: 11107079]
3. Isenberg BC, Williams C, Tranquillo RT. Small-diameter artificial arteries engineered in vitro. Circulation Research. 2006; 98(1):25–35. [PubMed: 16397155]
4. MacNeill BD, Pomerantseva I, Lowe HC, Oesterle SN, Vacanti JP. Toward a new blood vessel. Vascular Medicine. 2002; 7(3):241–246. [PubMed: 12553747]
5. Greisler HP. Interactions at the blood/material interface. Annals of Vascular Surgery. 1990; 4(1):98–103. [PubMed: 2297480]
6. Hoenig MR, Campbell GR, Rolfe BE, Campbell JH. Tissue-engineered blood vessels: alternative to autologous grafts? Arteriosclerosis, Thrombosis, and Vascular Biology. 2005; 25(6):1128–1134.
7. Dorigo W, Pulli R, Castelli P, Dorrucci V, Ferilli F, De Blasis G, Monaca V, Vecchiati E, Pratesi C. A multicenter comparison between autologous saphenous vein and heparin-bonded expanded polytetrafluoroethylene (ePTFE) graft in the treatment of critical limb ischemia in diabetics. J Vasc Surg. 2011; 54(5):1332–1338. [PubMed: 21840151]

8. Weinberg CB, Bell E. A blood vessel model constructed from collagen and cultured vascular cells. Science. 1986; 231(4736):397–400. [PubMed: 2934816]
9. Niklason LE, Gao J, Abbott WM, Hirschi KK, Houser S, Marini R, Langer R. Functional arteries grown in vitro. Science. 1999; 284(5413):489–493. [PubMed: 10205057]
10. Kaushal S, Amiel GE, Guleserian KJ, Shapira OM, Perry T, Sutherland FW, Rabkin E, Moran AM, Schoen FJ, Atala A, Soker S, Bischoff J, Mayer JE Jr. Functional small-diameter neovessels created using endothelial progenitor cells expanded ex vivo. Nat Med. 2001; 7(9):1035–1040. [PubMed: 11533707]
11. L'Heureux N, Dusserre N, Konig G, Victor B, Keire P, Wight TN, Chronos NA, Kyles AE, Gregory CR, Hoyt G, Robbins RC, McAllister TN. Human tissue-engineered blood vessels for adult arterial revascularization. Nat Med. 2006; 12(3):361–365. [PubMed: 16491087]
12. Dahl SLM, Kypson AP, Lawson JH, Blum JL, Strader JT, Li Y, Manson RJ, Tente WE, DiBernardo L, Hensley MT, Carter R, Williams TP, Prichard HL, Dey MS, Begelman KG, Niklason LE. Readily available tissue-engineered vascular grafts. Science Translational Medicine. 2011; 3(68): 68ra9–68ra9.
13. Wu W, Allen RA, Wang Y. Fast-degrading elastomer enables rapid remodeling of a cell-free synthetic graft into a neoartery. Nat Med. 2012; 18(7):1148–1153. [PubMed: 22729285]
14. Hashi CK, Zhu Y, Yang G-Y, Young WL, Hsiao BS, Wang K, Li S. Antithrombogenic property of bone marrow mesenchymal stem cells in nanofibrous vascular grafts. Proceedings of the National Academy of Sciences. 2007; 104(29):11915–11920.
15. Stitzel J, Liu J, Lee SJ, Komura M, Berry J, Soker S, Lim G, Van Dyke M, Czerw R, Yoo JJ, Atala A. Controlled fabrication of a biological vascular substitute. Biomaterials. 2006; 27(7):1088–1094. [PubMed: 16131465]
16. Ma Z, Kotaki M, Inai R, Ramakrishna S. Potential of nanofiber matrix as tissue-engineering scaffolds. Tissue Engineering. 2005; 11(1–2):101–109. [PubMed: 15738665]
17. Liang D, Hsiao BS, Chu B. Functional electrospun nanofibrous scaffolds for biomedical applications. Advanced Drug Delivery Reviews. 2007; 59(14):1392–1412. [PubMed: 17884240]
18. Grasl C, Bergmeister H, Stoiber M, Schima H, Weigel G. Electrospun polyurethane vascular grafts: In vitro mechanical behavior and endothelial adhesion molecule expression. Journal of Biomedical Materials Research Part A. 2010; 93A(2):716–723.
19. Bergmeister H, Grasl C, Walter I, Plasenzotti R, Stoiber M, Schreiber C, Losert U, Weigel G, Schima H. Electrospun small-diameter polyurethane vascular grafts: ingrowth and differentiation of vascular-specific host cells. Artificial Organs. 2012; 36(1):54–61. [PubMed: 21848935]
20. Feng Y, Tian H, Tan M, Zhang P, Chen Q, Liu J. Surface modification of polycarbonate urethane by covalent linkage of heparin with a PEG spacer. Transactions of Tianjin University. 2013; 19(1): 58–65.
21. Tiwari A, Salacinski H, Seifalian AM, Hamilton G. New prostheses for use in bypass grafts with special emphasis on polyurethanes. Vascular. 2002; 10(3):191–197.
22. Pinchuk L. A review of the biostability and carcinogenicity of polyurethanes in medicine and the new generation of 'biostable' polyurethanes. J Biomater Sci Polym Ed. 1994; 6(3):225–267. [PubMed: 7986779]
23. Szycher M, Reed A, Siciliano A. In vivo testing of a biostable polyurethane. J Biomater Appl. 1991; 6(2):110–130. [PubMed: 1779410]
24. Zdrahala R. Small caliber vascular grafts. Part II: Polyurethanes revisited. J Biomater Appl. 1996; 11(1):37–61. [PubMed: 8872599]
25. Szelest-Lewandowska A, Masiulanis B, Szymonowicz M, Pielka S, Paluch D. Modified polycarbonate urethane: synthesis, properties and biological investigation in vitro. J Biomed Mater Res A. 2007; 82(2):509–520. [PubMed: 17530635]
26. Guo J, Zhao M, Ti Y, Wang B. Study on structure and performance of polycarbonate urethane synthesized via different copolymerization methods. Journal of Materials Science. 2007; 42(14): 5508–5515.
27. Khan I, Smith N, Jones E, Finch DS, Cameron RE. Analysis and evaluation of a biomedical polycarbonate urethane tested in an in vitro study and an ovine arthroplasty model. Part I: materials selection and evaluation. Biomaterials. 2005; 26(6):621–631. [PubMed: 15282140]

28. Nakagawa Y, Ota K, Sato Y, Teraoka S, Agishi T. Clinical trial of new polyurethane vascular grafts for hemodialysis: compared with expanded polytetrafluoroethylene grafts. Artif Organs. 1995; 19(12):1227–1232. [PubMed: 8967879]
29. Walpoth B, Rogulenko R, Tikhvinskaia E, Gogolewski S, Schaffner T, Hess O, Althaus U. Improvement of patency rate in heparin-coated small synthetic vascular grafts. Circulation. 1998; 98(19 Suppl):II319–II323. [PubMed: 9852921]
30. Jeschke M, Hermanutz V, Wolf S, Köveker G. Polyurethane vascular prostheses decreases neointimal formation compared with expanded polytetrafluoroethylene. J Vasc Surg. 1999; 29(1): 168–176. [PubMed: 9882801]
31. Aldenhoff YBJ, van der Veen FH, ter Woorst J, Habets J, Poole–Warren LA, Koole LH. Performance of a polyurethane vascular prosthesis carrying a dipyridamole (Persantin®) coating on its lumenal surface. Journal of Biomedical Materials Research. 2001; 54(2):224–233. [PubMed: 11093182]
32. Tai NR, Salacinski HJ, Edwards A, Hamilton G, Seifalian AM. Compliance properties of conduits used in vascular reconstruction. British Journal of Surgery. 2000; 87(11):1516–1524. [PubMed: 11091239]
33. Salacinski HJ, Goldner S, Giudiceandrea A, Hamilton G, Seifalian AM, Edwards A, Carson RJ. The mechanical behavior of vascular grafts: a review. Journal of Biomaterials Applications. 2001; 15(3):241–278. [PubMed: 11261602]
34. Hirsh J, Anand SS, Halperin JL, Fuster V. Guide to anticoagulant therapy: Heparin: a statement for healthcare professionals from the American Heart Association. Circulation. 2001; 103(24):2994–3018. [PubMed: 11413093]
35. Capila I, Linhardt R. Heparin-protein interactions. Angew Chem Int Ed Engl. 2002; 41(3):391–412. [PubMed: 12491369]
36. Janairo RRR, Henry JJD, Lee BL, Hashi CK, Derugin N, Lee R, Li S. Heparin-modified small-diameter nanofibrous vascular grafts. NanoBioscience, IEEE Transactions on. 2012; 11(1):22–27.
37. Alferiev IS, Connolly JM, Stachelek SJ, Ottey A, Rauova L, Levy RJ. Surface heparinization of polyurethane via bromoalkylation of hard segment nitrogens. Biomacromolecules. 2005; 7(1):317–322.
38. Lu Y, Shen L, Gong F, Cui J, Rao J, Chen J, Yang W. Polycarbonate urethane films modified by heparin to enhance hemocompatibility and endothelialization. Polymer International. 2012; 61(9): 1433–1438.
39. Ku SH, Park CB. Human endothelial cell growth on mussel-inspired nanofiber scaffold for vascular tissue engineering. Biomaterials. 2010; 31(36):9431–9437. [PubMed: 20880578]
40. Shin YM, Lee YB, Kim SJ, Kang JK, Park J-C, Jang W, Shin H. Mussel-inspired immobilization of vascular endothelial growth factor (VEGF) for enhanced endothelialization of vascular grafts. Biomacromolecules. 2012; 13(7):2020–2028. [PubMed: 22617001]
41. Tsai W-B, Chen W-T, Chien H-W, Kuo W-H, Wang M-J. Poly(dopamine) coating of scaffolds for articular cartilage tissue engineering. Acta Biomaterialia. 2011; 7(12):4187–4194. [PubMed: 21839186]
42. Tsai W-B, Chen W-T, Chien H-W, Kuo W-H, Wang M-J. Poly(dopamine) coating to biodegradable polymers for bone tissue engineering. Journal of Biomaterials Applications. 2014; 28(6):837–848. [PubMed: 24381201]
43. Kawamoto Y, Nakao A, Ito Y, Wada N, Kaibara M. Endothelial cells on plasma-treated segmented polyurethane. J Mater Sci Mater Med. 1997; 8(9):551–557. [PubMed: 15348707]
44. Bae J-S, Seo E-J, Kang I-K. Synthesis and characterization of heparinized polyurethanes using plasma glow discharge. Biomaterials. 1999; 20(6):529–537. [PubMed: 10213356]
45. Lee BL-P, Jeon H, Wang A, Yan Z, Yu J, Grigoropoulos C, Li S. Femtosecond laser ablation enhances cell infiltration into three-dimensional electrospun scaffolds. Acta Biomaterialia. 2012; 8(7):2648–2658. [PubMed: 22522128]
46. Hashi CK, Derugin N, Janairo RRR, Lee R, Schultz D, Lotz J, Li S. Antithrombogenic modification of small-diameter microfibrous vascular grafts. Arteriosclerosis, Thrombosis, and Vascular Biology. 2010; 30(8):1621–1627.

47. Zhu Y, Gao C, He T, Shen J. Endothelium regeneration on luminal surface of polyurethane vascular scaffold modified with diamine and covalently grafted with gelatin. Biomaterials. 2004; 25(3): 423–430. [PubMed: 14585690]
48. Lee BL-P, Tang Z, Wang A, Huang F, Yan Z, Wang D, Chu JS, Dixit N, Yang L, Li S. Synovial stem cells and their responses to the porosity of microfibrous scaffold. Acta Biomaterialia. 2013; 9(7):7264–7275. [PubMed: 23523935]
49. Yu J, Wang A, Tang Z, Henry J, Li-Ping Lee B, Zhu Y, Yuan F, Huang F, Li S. The effect of stromal cell-derived factor-1α/heparin coating of biodegradable vascular grafts on the recruitment of both endothelial and smooth muscle progenitor cells for accelerated regeneration. Biomaterials. 2012; 33(32):8062–8074. [PubMed: 22884813]
50. Lee H, Dellatore SM, Miller WM, Messersmith PB. Mussel-inspired surface chemistry for multifunctional coatings. Science. 2007; 318(5849):426–430. [PubMed: 17947576]
51. Murugesan S, Xie J, Linhardt R. Immobilization of heparin: approaches and applications. Curr Top Med Chem. 2008; 8(2):80–100. [PubMed: 18289079]
52. Begovac PC, Thomson RC, Fisher JL, Hughson A, Gällhagen A. Improvements in GORE-TEX® vascular graft performance by Carmeda® bioactive surface heparin immobilization. European Journal of Vascular and Endovascular Surgery. 2003; 25(5):432–437. [PubMed: 12713782]
53. Chuang T-W, Masters KS. Regulation of polyurethane hemocompatibility and endothelialization by tethered hyaluronic acid oligosaccharides. Biomaterials. 2009; 30(29):5341–5351. [PubMed: 19577800]
54. Noel S, Liberelle B, Robitaille L, De Crescenzo G. Quantification of primary amine groups available for subsequent biofunctionalization of polymer surfaces. Bioconjugate Chemistry. 2011; 22(8):1690–1699. [PubMed: 21736371]
55. Wong KKH, Hutter JL, Zinke-Allmang M, Wan W. Physical properties of ion beam treated electrospun poly(vinyl alcohol) nanofibers. European Polymer Journal. 2009; 45(5):1349–1358.
56. Gibeop N, Lee DW, Prasad CV, Toru F, Kim BS, Song JI. Effect of plasma treatment on mechanical properties of jute fiber/poly (lactic acid) biodegradable composites. Advanced Composite Materials. 2013; 22(6):389–399.
57. He W, Yong T, Teo WE, Ma Z, Ramakrishna S. Fabrication and endothelialization of collagen-blended biodegradable polymer nanofibers: potential vascular graft for blood vessel tissue engineering. Tissue Engineering. 2005; 11(9–):1574–1588. [PubMed: 16259611]
58. Riesenfeld J, Olsson P, Sanchez J, Mollnes T. Surface modification with functionally active heparin. Med Device Technol. 1995; 6(2):24–31.
59. Bernfield M, Götte M, Park PW, Reizes O, Fitzgerald ML, Lincecum J, Zako M. Functions of cell surface heparan sulfate proteoglycans. Annual Review of Biochemistry. 1999; 68(1):729–777.
60. Powell AK, Yates EA, Fernig DG, Turnbull JE. Interactions of heparin/heparan sulfate with proteins: Appraisal of structural factors and experimental approaches. Glycobiology. 2004; 14(4): 17R–30R.
61. Kurpinski KT, Stephenson JT, Janairo RR, Lee H, Li S. The effect of fiber alignment and heparin coating on cell infiltration into nanofibrous PLLA scaffolds. Biomaterials. 2010; 31(13):3536–3542. [PubMed: 20122725]
62. Badylak SF, Valentin JE, Ravindra AK, McCabe GP, Stewart-Akers AM. Macrophage phenotype as a determinant of biologic scaffold remodeling. Tissue Engineering Part A. 2008; 14(11):1835–1842. [PubMed: 18950271]

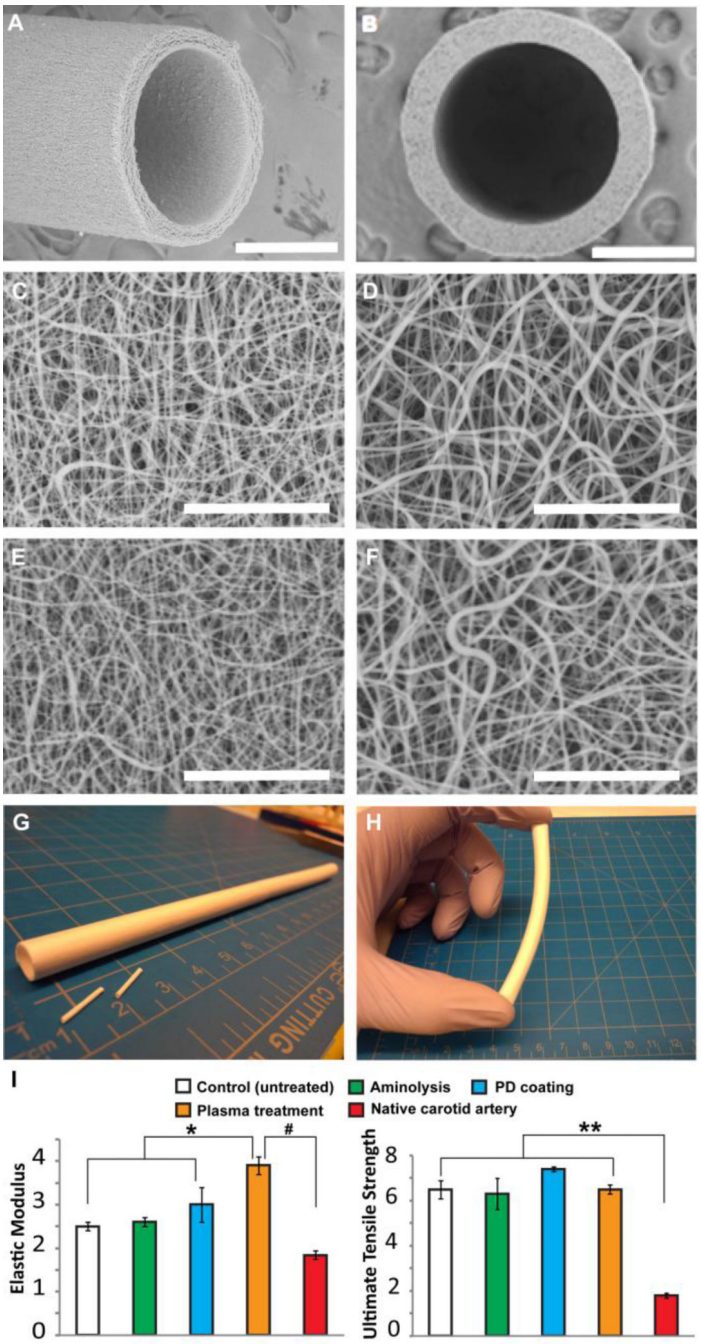

Figure 1.

Structural and mechanical characterization of nanofibrous PCU vascular graft. Scanning electron microscopy (SEM) images taken from (A) side and (B) top view of an electrospun PCU vascular graft. Structure of nanofibers in the (C) inner (luminal) and (D) outer surface of the vascular graft before the plasma treatment; structure of nanofibers in the (E) inner and (F) outer surface of the vascular graft after the plasma treatment. (G) Nanofibrous PCU vascular grafts of various inner diameters (i.e. 1-mm and 6-mm) were fabricated to demonstrate the versatility of electrospinning setup. (H) Bending of a 6 mm-diameter PCU

graft to confirm desired mechanical property. (I) Comparison of elastic modulus and ultimate tensile strength (UTS) among control (untreated), aminolyzed, polydopamine (PD)-coated, plasma-treated grafts and native common carotid arteries (n=5). *, #, ** indicate significant difference ($P<0.05$). Scale bar = 500 μm in A, B; scale bar = 30 μm in C, D, E, F.

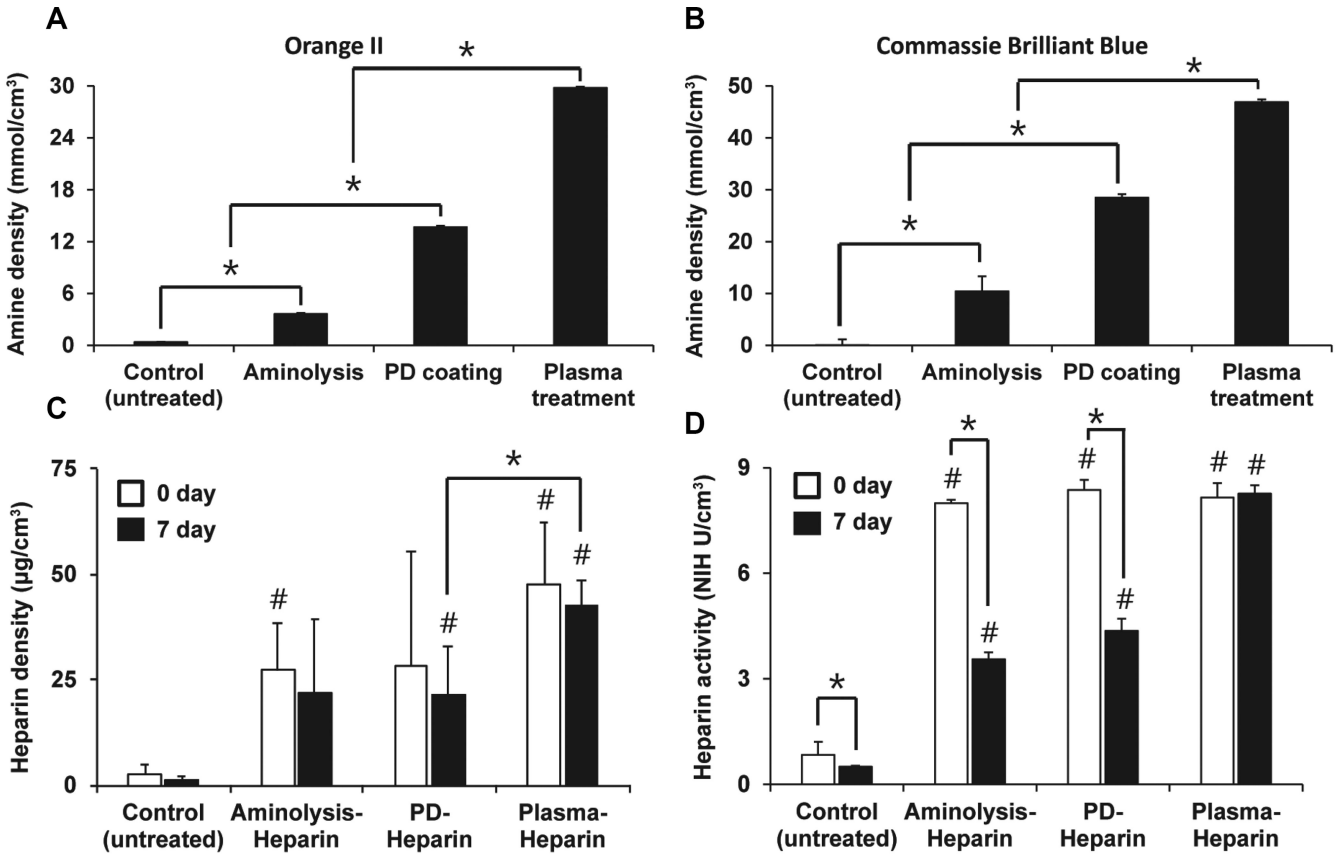

Figure 2.

Chemical characterization and comparison of surface modifications and heparin conjugation on the surface of nanofibrous PCU vascular graft. Surface density of functional amine groups as introduced via aminolysis, polydopamine (PD) coating, and plasma treatment were quantified using (A) Orange II and (B) Coomassie Brilliant Blue (CBB) dye staining (n=3). (C) Toluidine blue assay was used to verify the presence of conjugated heparin and compare its stability after 1 week (n=3). # indicates significant difference (P<0.05) compared to control (untreated) grafts at respective time point; * indicates significant difference (P<0.05) between the two groups. (D) The maintenance and retention of the anti-thrombogenic activity of immobilized heparin on the graft surface was quantified using anti-thrombin-III (n=3). # indicates significant difference (P<0.05) compared to control (untreated) grafts at respective time point; * indicates significant difference (P<0.05) between the two time points of the same group.

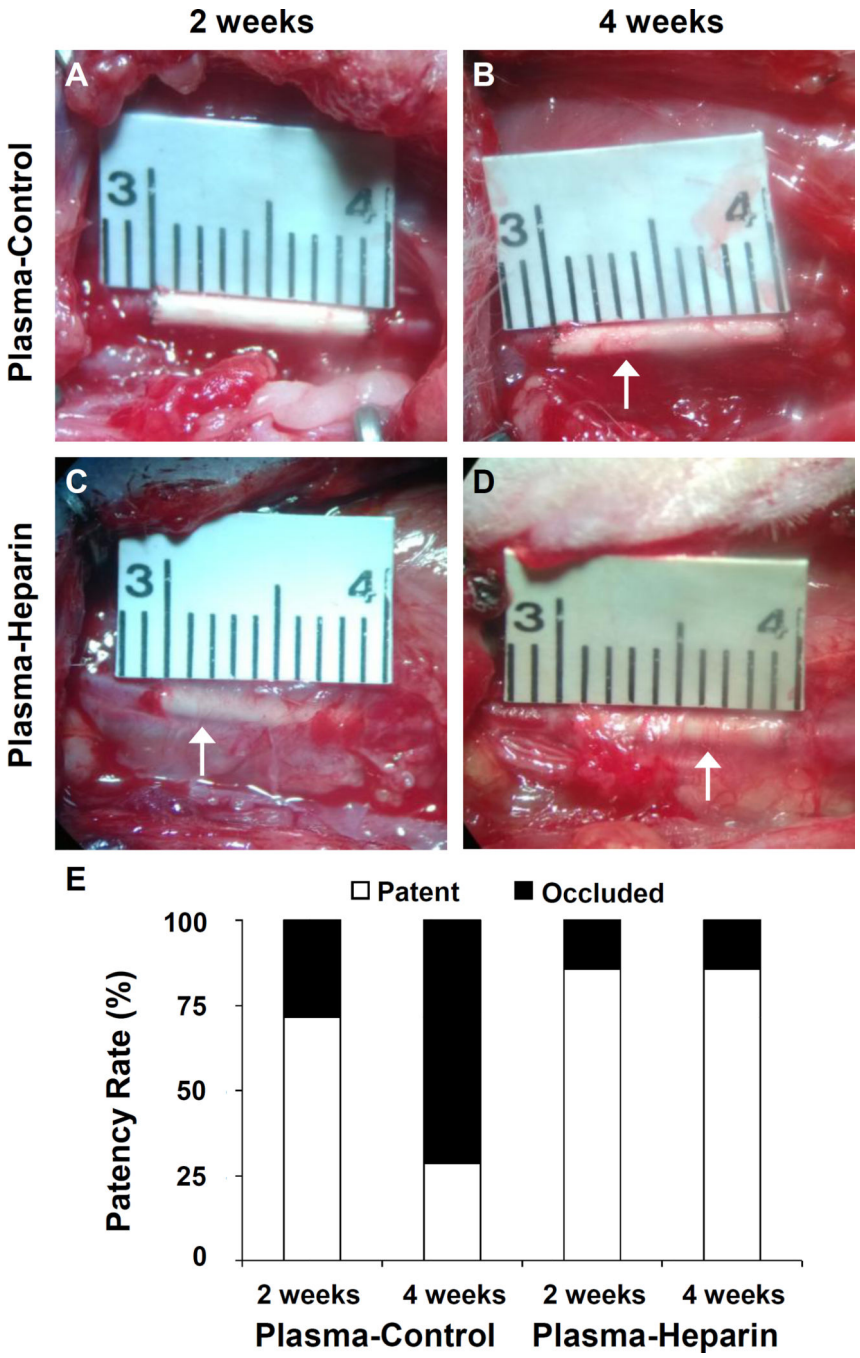

Figure 3.

Graft explantation and patency of the grafts. Representative image of a (A) 2-week and (B) 4-week plasma-control graft *in situ* taken immediately prior to explantation. Representative image of a (C) 2-week and (D) 4-week plasma-heparin graft *in situ* taken immediately prior to explantation. White arrows indicate noticeable microvessels and vascularization in the surrounding tissue of the grafts. Scale bar is as denoted in A–D. (E) Patency rates of the grafts after 2 weeks and 4 weeks *in vivo* were recorded and compared. Each group at each time point included 7 animals (n=7).

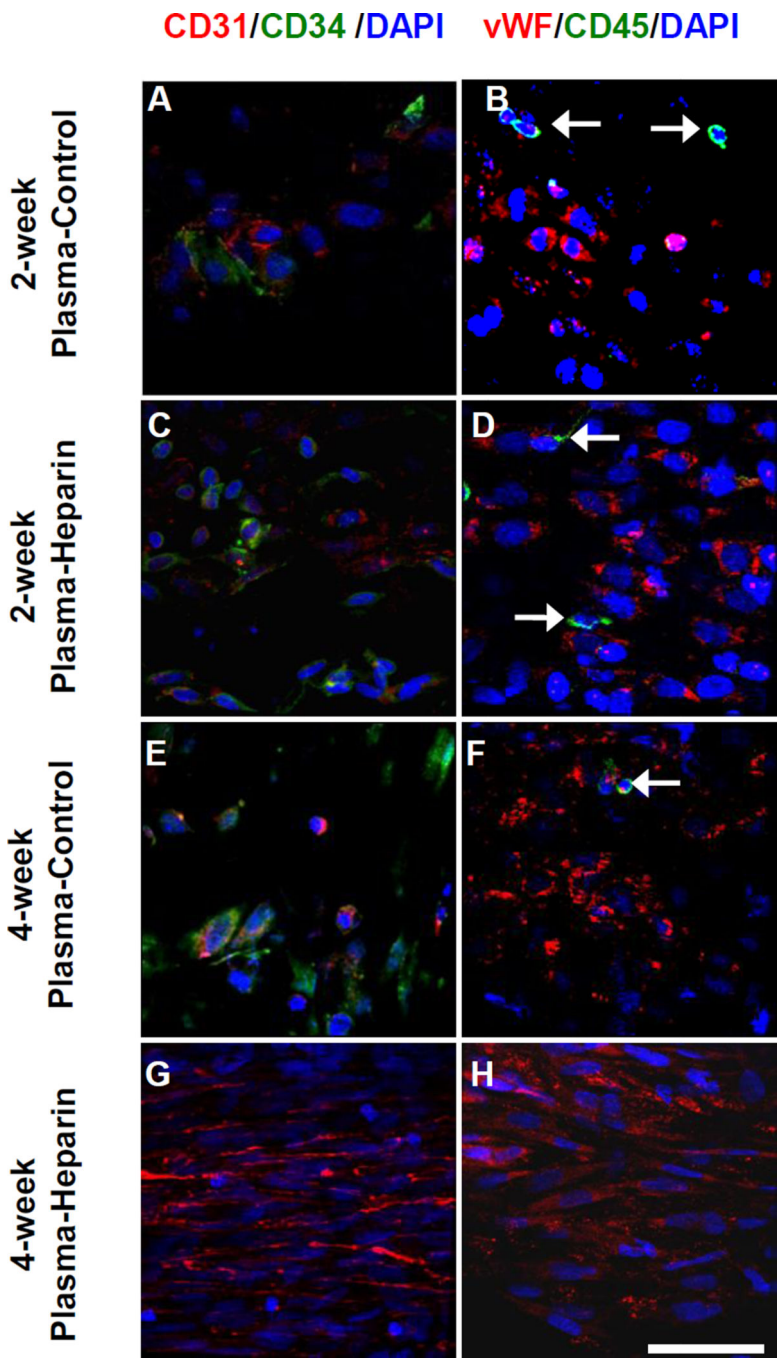

Figure 4.

En face immunostaining of PCU plasma-control and plasma-heparin grafts after 2 and 4 weeks *in vivo*. *En face* immunostaining for CD31 (red) with CD34 (green) and vWF (red) with CD45 (green) of patent (A, B) 2-week plasma-control, (C, D) 2-week plasma-heparin, (E, F) 4-week plasma-control and (G, H) 4-week plasma-heparin grafts were performed. White arrows indicate cells positive for CD45. Cell nuclei were stained using DAPI (blue). Scale bar = 50 μm.

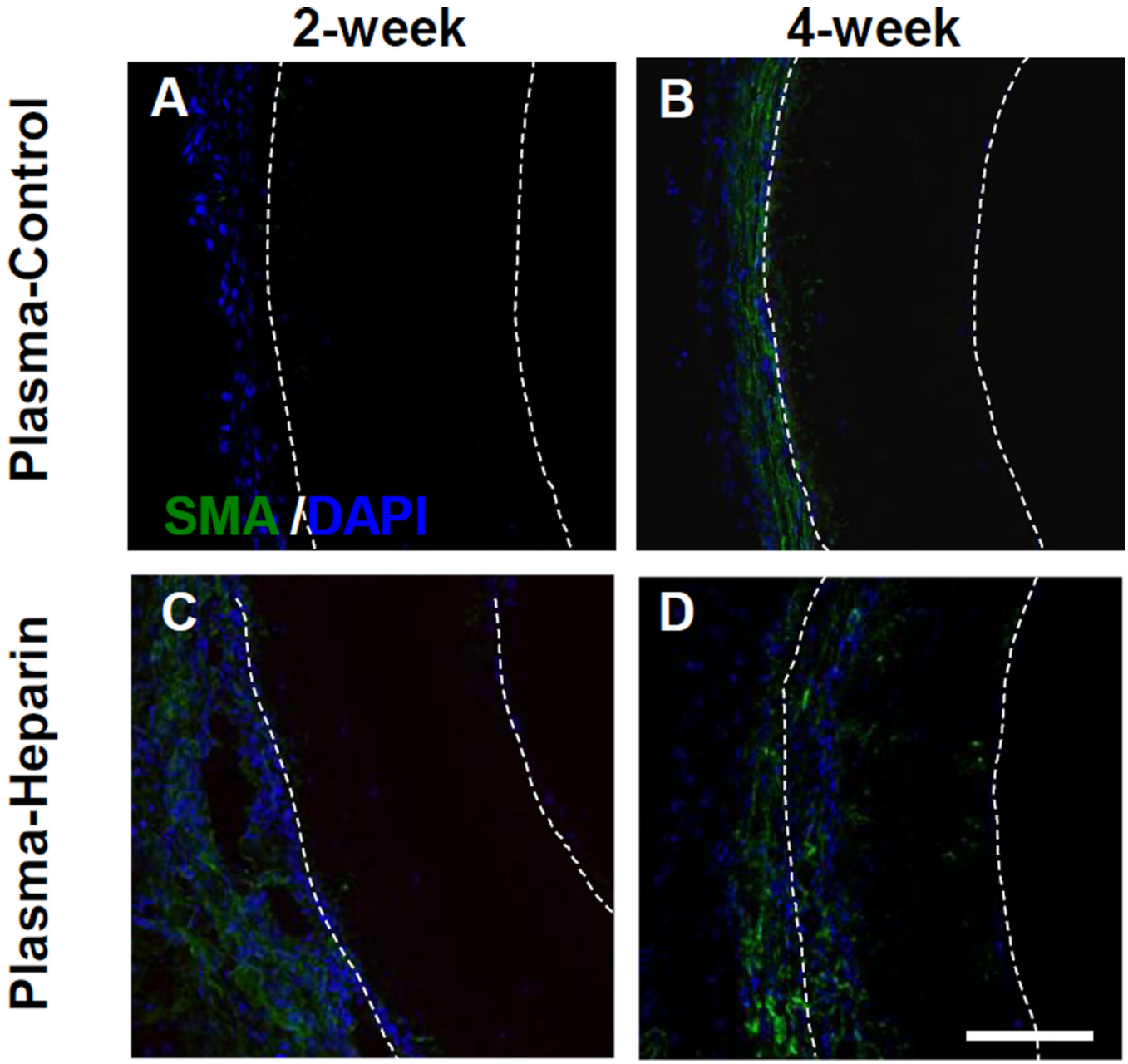

Figure 5.

Cross-section immunostaining of PCU plasma-control and plasma-heparin grafts after 2 and 4 weeks *in vivo*. Immunostaining for SMA (green) of the cross-sections obtained from the vascular graft of the plasma-control and plasma-heparin grafts after 2 (A, C) and 4 (B, D) weeks *in vivo* was performed. White dashed lines delineate the border of the graft wall. Cell nuclei were stained using DAPI (blue). Scale bar = 100 μm.

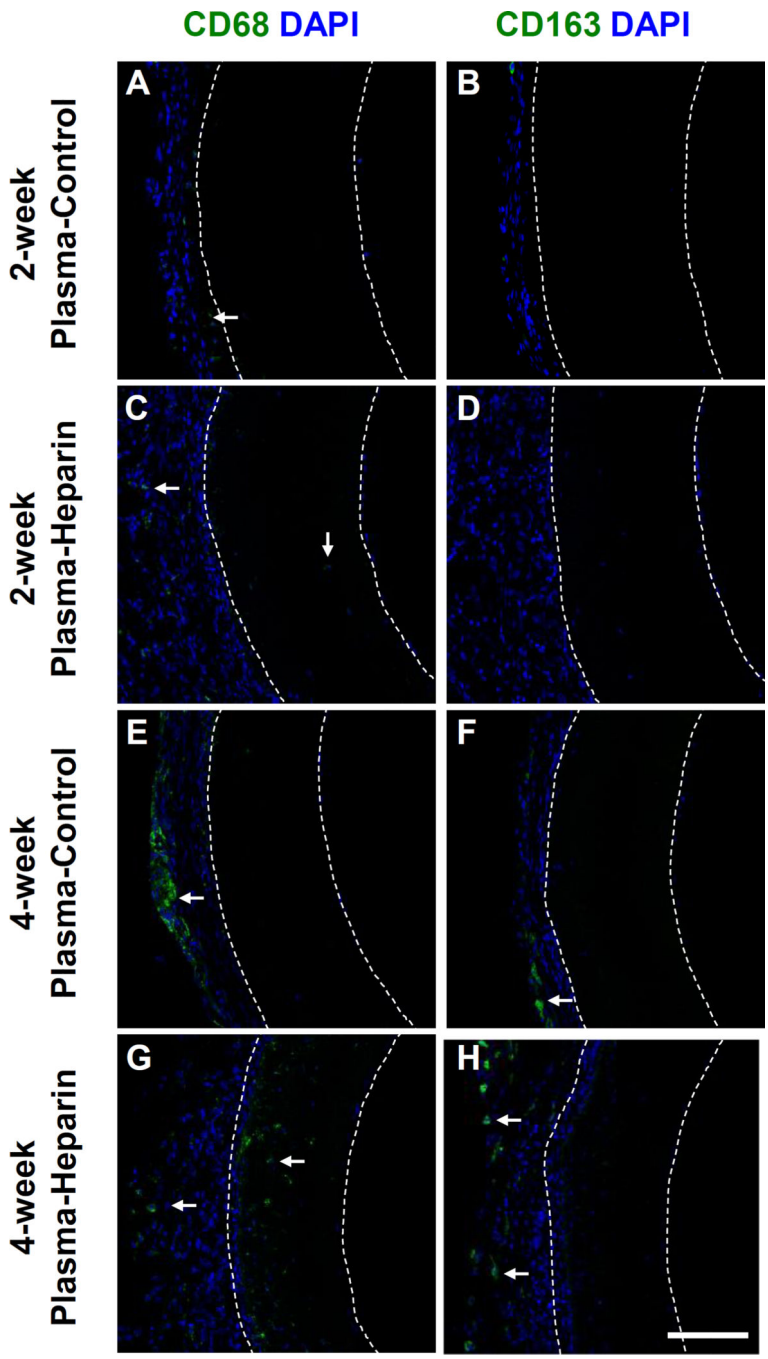

Figure 6.

Inflammatory response of PCU plasma-control and plasma-heparin grafts after 2 and 4 weeks *in vivo*. Immunostaining for (A, C, E, G) CD68 and (B, D, F, H) CD163 of the cross-sections obtained from the vascular graft of the plasma-control and plasmaheparin grafts after 2 and 4 weeks *in vivo* was performed. White arrows indicate cells positive for CD68 and CD163, respectively, within the graft wall. White dashed lines delineate the border of the graft wall. Cell nuclei were stained using DAPI (blue). Scale bar = 100 μm.